





Proceedings Article

Model-based voltage predictions for arbitrary waveform excitation in Magnetic Particle Imaging

Justin Ackers ^{a,*} · Fabian Mohn ^{c,d} · Niklas Hackelberg ^{c,d} · Tobias Knopp ^{c,d} · Thorsten M. Buzug ^{a,b} · Matthias Graeser ^{a,b,*}

^aFraunhofer Research Institution for Individualized and Cell-Based Medical Engineering IMTE, Lübeck, Germany

^bInstitute of Medical Engineering, University of Lübeck, Lübeck, Germany

^cSection for Biomedical Imaging, University Medical Center Hamburg-Eppendorf, Hamburg, Germany

^dInstitute for Biomedical Imaging, Hamburg University of Technology, Hamburg, Germany

*Corresponding author, email: {justin.ackers, matthias.graeser}@imte.fraunhofer.de

© 2023 Ackers *et al.*; licensee Infinite Science Publishing GmbH

This is an Open Access article distributed under the terms of the Creative Commons Attribution License (<http://creativecommons.org/licenses/by/4.0>), which permits unrestricted use, distribution, and reproduction in any medium, provided the original work is properly cited.

Abstract

In recent works, arbitrary waveform or pulsed excitation in Magnetic Particle Imaging (MPI) was proposed to offer better resolution and sensitivity. Generating these excitation fields poses a new challenge in MPI hardware design. This work proposes a method which models the excitation chain as a linear system and predicts the required input voltage for the desired output field. The initial prediction is then iteratively improved to compensate for inaccuracies of the model. The method is demonstrated to achieve accurate field waveforms in both linear and slew rate limited regions of the amplifier.

1. Introduction

In MPI the spatial concentration of superparamagnetic iron oxide nanoparticles (SPIONs) is measured by the particles non-linear response to a superposition of different magnetic fields, used for excitation (drive field) and spatial selection (selection field). Typically, MPI systems implement sinusoidal waveforms to drive the SPIONs into saturation, but recently other waveform shapes have been proposed by Tay *et al.* [1] and used in a multitude of applications [2, 3]. Currently, arbitrary waveforms are under investigation to improve resolution or sensitivity by analyzing different tracers and trajectories with a magnetic particle spectrometer (MPS). An arbitrary waveform system faces several challenges in instrumentation, like the elimination of direct feedthrough of the excitation field, which can not be filtered due to the broad-

band excitation, or the non-resonant transmit circuit that puts high constraints on amplifiers and coil design. Opposed to conventional fixed frequency MPI, the inductive load is typically directly attached to the amplifier with no capacitive impedance matching network. One way to realize arbitrary waveforms is to use the controlled current mode built into some power amplifiers, which uses an analog, user-tuneable feedback loop to enable a transconductance mode. The drawback of this is that the feedback needs to be tuned for a specific load and pulse height and the available bandwidth is restricted by the amplifier to avoid instability. In order to use the full bandwidth and maximum slew rate of an amplifier, the approach in this work uses the standard voltage amplification mode and regards amplifier and transmit coil as a single unit for which the optimal voltage is determined. Based on feedback from a current monitor, an iterative

procedure maps the desired periodic output current in the coil to the required amplifier voltage. By differentiating between a linear case and a non-linear case, waveforms can be optimized even in proximity to maximum device specifications where non-linear behaviour dominates.

II. Material and Methods

The basic components of the excitation pipeline used in an arbitrary waveform MPS are shown in the block diagram in Figure 1. A data acquisition unit (DAQ) outputs a voltage which is amplified by the power amplifier and directly applied to the coil, resulting in the desired output quantity: the magnetic field inside the sample chamber. To enable the control of the magnetic field a feedback signal with information about the current output of the amplifier is returned to the DAQ.

By assuming linearity in all components and due to the periodic nature of all used signals, the block diagram can be translated into a system of transfer functions, switching to a frequency space formulation of the important quantities \hat{V}_{tx} (output voltage of DAQ), \hat{V}_{ref} (reference voltage), and the one dimensional magnetic field \hat{B}_{coil} , oriented along the principle axis of the coil in the sample chamber. The amplifier has an idealized transfer function characterized by its voltage gain G_{amp} . The transfer function of the coil is defined by its complex impedance $Z_{coil} = R + j\omega L$, which is modeled by an ideal inductor in series with a resistor and maps the incoming voltage to the current. The second component of the coil is its scalar sensitivity, i.e. the generated magnetic field per unit current P_{coil} in its center. For the small sample chamber of the MPS, a homogeneous sensitivity is assumed. Regarding the reference monitor, the frequency dependent transmit transfer function of the excitation field to voltage output can be acquired through a calibration measurement, but in this work is only approximated by a scalar value G_{ref} with unit VT^{-1} . To achieve the desired field inside the sample chamber, the following general procedure is used: First, the model of the excitation pipeline is inverted to generate an initial prediction for \hat{V}_{tx} for a desired excitation field \hat{B}_{goal} :

$$\hat{V}_{tx_0} = \hat{B}_{goal} \cdot P_{coil}^{-1} \cdot Z_{coil} \cdot G_{amp}^{-1}. \quad (1)$$

To ensure that the transmit voltage does not contain frequencies that the amplifier can not produce, \hat{B}_{goal} is low-pass filtered with a cutoff frequency of 500 kHz. This voltage is then transmitted, the reference signal recorded, and then used to update the voltage that should be transmitted in the next step $i + 1$, compensating any inaccuracies of the model:

$$\hat{V}_{tx_{i+1}} = \hat{V}_{tx_i} \cdot \frac{\hat{B}_{goal}}{\hat{V}_{ref_i} \cdot G_{ref}^{-1}}. \quad (2)$$

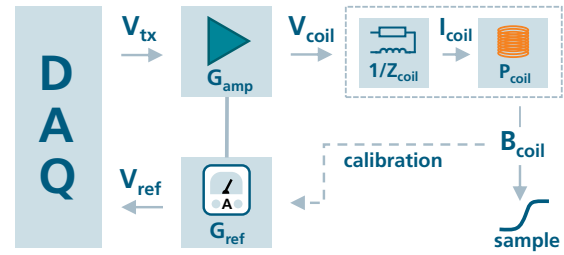


Figure 1: Block diagram of the excitation pipeline. The DAQ generates a voltage which is amplified and directly applied to the coil, which results in a current, that in turn generates the excitation field. The DAQ receives a feedback signal from the current monitor of the amplifier to adapt the next iteration.

This iterative process is repeated until the deviation of the measured field to the desired field is below a user defined threshold. The update procedure enables the model to overcome small non-linearities, since each step linearizes the system at that specific operating point.

However, the linear model is not sufficient anymore in the case that the calculated voltage would drive the amplifier into its voltage or slew rate limit, which is the case when a square wave output current is desired for pulsed magnetic fields. Therefore, a distinction is made between the linear case and the slew rate limited, non-linear, case. For the latter a different procedure has to be followed if an iteration of the linear model is detected to exceed the specifications of the amplifier.

When the amplifier is in proximity of its slew rate limit, a square voltage pulse at the input gets flattened into a triangular voltage at the output (see Figure 2 (b)). With a slope equal to the amplifier slew rate, this triangular voltage results in the highest achievable current slew rate into the inductive load with this amplifier. In order to achieve as rectangular a current waveform as possible, a transmit waveform is generated, which has a pulse of maximum amplifier voltage for a variable duration, maximizing the current rise within the coil. After the current is achieved the voltage drops to the required voltage for the desired plateau of the square wave. The optimal duration for the short maximum voltage pulse should result in the current reaching the plateau with minimal over- or undershoot and can be found by a procedure similar to the linear case: an initial estimate for the pulse duration is generated by solving the differential equation of the current in the coil for an ideally slew rate limited (i.e. triangular) voltage impulse. Afterwards, the impulse duration can be iteratively adjusted to achieve the best fit to the desired rectangular wave.

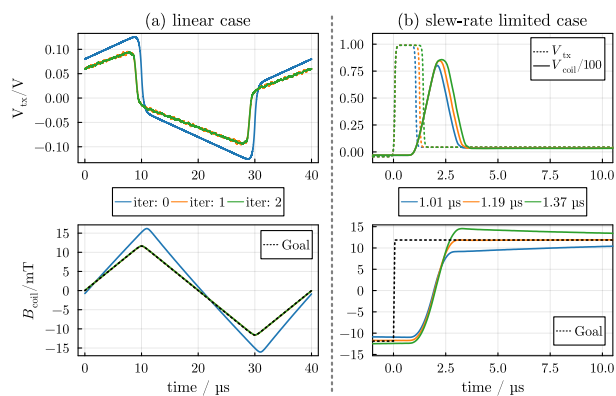


Figure 2: Transmitted voltages and resulting excitation fields for individual optimization steps in (a) the linear case and (b) the slew rate limited case.

III. Experiments and results

To evaluate the proposed current control method, the basic structure of Figure 1 was implemented using a Red-Pitaya based DAQ, a Hubert A1110-16-E power amplifier and a field generating coil with $11.1 \mu\text{H}$ and 0.85Ω . The DAQ software stack was extended to enable the output of arbitrary waveforms in addition to the already implemented sinusoidal waveforms [4]. To evaluate the presented current control method, multiple triangular and square waveforms with different amplitudes and frequencies were generated. As a representative example the results of the individual iterations for a triangle with 12 mT and 25 kHz are shown in Figure 2 (a), with the input voltages of each iteration at the top and the resulting fields below. It can be observed that the result for the initial prediction is already close to the desired output signal, showing the good general approximation of the linear model. Furthermore, the second iteration achieves the goal of correcting the remaining errors of the model, like underestimated gain or non-linearities in the load model, resulting in very low differences in the measured current to the desired current. The following iterations only change the output slightly.

The second measurement (b) shows the results for maximum input pulses for different pulse widths, including the optimal pulse time, to generate steep field pulses in the coil. On the top right, the transmitted voltage and the corresponding amplifier voltage show how the slew rate limit affects the actual transmitted signal. The bottom right shows the resulting pulses for different time steps, demonstrating the different over- and undershoot effects, with the optimal time of $1.19 \mu\text{s}$ achieving a fast jump from -12 mT to 12 mT with minimal overshoot. This timing is consistent for all frequencies of square waves, since the only difference is the duration of the constant part between the flanks.

IV. Discussion and Outlook

The results demonstrate the ability of the presented method to create arbitrary periodic fields in a largely inductive load while using the full capabilities of the amplifier. To ensure that the presented method can reliably control the excitation field, the calibration of the feedback path from field to reference signal is essential. Small inaccuracies can lead to imperfect detection of the steep current flanks and the result would be an inaccurate excitation field. First, the scalar value G_{ref} should be extended into a frequency dependent transfer function to calibrate any frequency dependent behaviour of the current measurement. And second, the frequency dependent behaviour of the DAQ input should be considered, since slight deviations in V_{ref} rise time were observed between measurements with the DAQ unit and an external oscilloscope.

Once it is embedded in a software framework [5], the presented approach yields maximum flexibility for different MPI systems and arbitrary waveform excitation and sequences.

Acknowledgments

Research funding: Fraunhofer IMTE is supported by the EU (EFRE) and the State Schleswig-Holstein, Germany (Project: Diagnostic and therapy methods for Individualized Medical Technology (IMTE) – Grant: 124 20 002 / LPW-E1.1.1/1536).

Author's statement

Conflict of interest: Authors state no conflict of interest.

References

- [1] Z. W. Tay, D. Hensley, J. Ma, P. Chandrasekharan, B. Zheng, P. Goodwill, and S. Conolly. Pulsed Excitation in Magnetic Particle Imaging. *IEEE Transactions on Medical Imaging*, 38(10):2389–2399, 2019, Publisher: Institute of Electrical and Electronics Engineers (IEEE). doi:[10.1109/tmi.2019.2898202](https://doi.org/10.1109/tmi.2019.2898202).
- [2] D. Pantke, N. Holle, A. Mogarkar, M. Straub, and V. Schulz. Multifrequency magnetic particle imaging enabled by a combined passive and active drive field feed-through compensation approach. *Medical physics*, 46(9):4077–4086, 2019, doi:[10.1002/mp.13650](https://doi.org/10.1002/mp.13650).
- [3] F. Mohn, T. Knopp, M. Boberg, F. Thieben, P. Szwargulski, and M. Graeser. System Matrix based Reconstruction for Pulsed Sequences in Magnetic Particle Imaging. *IEEE Transactions on Medical Imaging*, pp. 1–1, 2022, doi:[10.1109/TMI.2022.3149583](https://doi.org/10.1109/TMI.2022.3149583).
- [4] N. Hackelberg, J. Schumacher, M. Graeser, and T. Knopp. A Flexible High-Performance Signal Generation and Digitization Platform based on Low-Cost Hardware. *International Journal on Magnetic Particle Imaging*, 8(1 Suppl 1), 2022, Publisher: International Journal on Magnetic Particle Imaging. doi:[10.18416/IJMPI.2022.2203063](https://doi.org/10.18416/IJMPI.2022.2203063).
- [5] N. Hackelberg, J. Schumacher, J. Ackers, M. Möddel, F. Foerger, M. Graeser, and T. Knopp. MPIMeasurements.jl: An Extensible Julia Framework for Composable Magnetic Particle Imaging Devices. *International Journal on Magnetic Particle Imaging*, 9(1 Suppl 1), 2023.